Published in final edited form as:
J Mol Cell Cardiol. 2008 May ; 44(5): 891–904. doi:10.1016/j.yjmcc.2008.02.274.

Allele and species dependent contractile defects by restrictive and hypertrophic cardiomyopathy-linked troponin I mutants

Jennifer Davis, **Haitao Wen**, **Terri Edwards**, and **Joseph M. Metzger**
Department of Molecular and Integrative Physiology, University of Michigan, Ann Arbor, Michigan, USA

Abstract

Restrictive cardiomyopathy (RCM) is a debilitating disease characterized by impaired ventricular filling, reduced ventricular volumes, and severe diastolic dysfunction. Hypertrophic cardiomyopathy (HCM) is characterized by ventricular hypertrophy and heightened risk of premature sudden cardiac death. These cardiomyopathies can result from mutations in the same gene that encodes for cardiac troponin I (cTnI). Acute genetic engineering of adult rat cardiac myocytes was used to ascertain whether primary physiologic outcomes could distinguish between RCM and HCM alleles at the cellular level. Co-transduction of cardiac myocytes with wild-type (WT) cTnI and RCM/HCM linked mutants in cTnI's inhibitory region (IR) demonstrated that WT cTnI preferentially incorporates into the sarcomere over IR mutants. The cTnI IR mutants exhibited minor effects in single, rodent, myocyte Ca^{2+}-activated tension assays yet prolonged relaxation and Ca^{2+} decay. RCM cTnI mutants in the helix-4/C-terminal region demonstrated a) hyper-sensitivity to Ca^{2+} under loaded conditions, b) slower myocyte mechanical relaxation and Ca^{2+} transient decay, c) frequency-dependent Ca^{2+}-independent diastolic tone, d) heightened myofilament incorporation and e) irreversible cellular contractile defects with acute diltiazem administration. For species comparison, a subset of cTnI mutants were tested in isolated adult rabbit cardiac myocytes. Here, RCM and HCM mutant cTnIs exerted similar effects of slowed sarcomere length relaxation and Ca^{2+} transient decay but did not show variable phenotypes by cTnI region. This study highlights cellular contractile defects by cardiomyopathy mutant cTnIs that are allele and species dependent. The species dependent results in particular raise important issues toward elucidating a unifying mechanistic pathway underling the inherited cardiomyopathies.

Keywords

inherited cardiomyopathy; cardiac troponin I; myocyte; contraction

1. Introduction

Inherited cardiomyopathies are disorders of the myocardium that represent a significant cause of morbidity and mortality [1]. Familial cardiomyopathies typically have an autosomal dominant pattern of inheritance and have been classified into several distinct disease entities

Contact: Joseph M. Metzger, Ph.D., 7730 Med Sci II, 1301 E. Catherine St., Ann Arbor, MI 48109-0622, Telephone: 734-763-0560, Fax: 734-647-6461, Email: metzgerj@umich.edu.

Disclosures None.

based on morphologic and functional criteria [1;2]. Hypertrophic cardiomyopathy (HCM) has a prevalence of 1 in 500 in the general population and is characterized by unexplained left ventricular hypertrophy, diastolic dysfunction, and a high incidence of sudden cardiac death [2–6]. In comparison, restrictive cardiomyopathy (RCM) is a rare, highly malignant heart muscle disease characterized by reduced compliance of the myocardium, impaired ventricular filling, and heightened diastolic dysfunction in the absence of ventricular hypertrophy [1;2;7;8]. The natural history of RCM can include early morbidity during childhood with the only treatment in that case being transplantation [7]. Both HCM and RCM can result from mutations in the same gene [9], *TNNI3*, which encodes for cardiac troponin I (cTnI). With the significant advances in both molecular cardiology and disease diagnosis, clinically stratifying patients into HCM or RCM categories has become challenging as the boundaries between these cardiomyopathic phenotypes are no longer clearly defined [1]. Therefore, the primary objectives of this study were two-fold: 1) to determine the direct physiologic effects of RCM and HCM linked mutant cTnI alleles on adult myocyte physiology and 2) to determine if these mutations can result in diverse cellular phenotypes akin to the clinically distinct organ level outcomes.

Cardiac troponin I is the inhibitory subunit of the thin filament regulatory protein troponin. Within the troponin complex, cTnI partners with troponin C (TnC), the Ca^{2+} binding subunit, and troponin T (TnT), the tropomyosin binding subunit, to regulate cardiac muscle contraction in response to Ca^{2+} [10;11]. Cardiac troponin I has been modeled as a Ca^{2+}-dependent molecular switch in the sarcomere. During diastole, cTnI interacts tightly with actin to block strong cross-bridge binding. As Ca^{2+} concentrations rise during systole, cTnI interacts with TnC, and ensuing conformational changes in the thin filament become permissive for active cross-bridge cycling [12]. High resolution atomic structures of troponin and detailed biophysical data [11;13–15] have identified cTnI's multi-domain secondary structure, which consists of four helices interspersed with several flexible linkers giving rise to six functional domains (Figure 1A). The identified RCM cTnI alleles [9] result in the following amino acid substitutions: L145Q, R146W, A172T, K179E, D191G, and R193H (based on the rodent amino acid sequence) that occupy several of cTnI's critical functional domains [12]. These include the inhibitory region (IR; residues 137–148), switch region (helices 3 and 4; residues 150–159 and 164–188), and C-terminus (residues 188–211, Figure 1A). Over 90% of identified HCM linked alleles result in amino acid substitutions that cluster within these same functional domains [16]. Thus, the mechanistic basis for how mutations in the same functional region of cTnI can result in diverse organ level phenotypes has remained elusive.

Of the known HCM linked cTnI mutants the R146G allele results in the greatest functional deficits relative to other known HCM causing cTnI mutations in both genetic and biochemical replacement models [17–20] and therefore R146G served as the archetype for HCM in this study. By contrast the primary physiologic consequence of most of the RCM mutant alleles remains poorly understood. While biochemical reconstitution models have shown that RCM cTnI alleles over sensitize the myofilament to Ca^{2+} in both tension and ATPase assays [17;20;21], a recent study using acute gene transfer to adult rodent cardiac myocytes with RCM R193H mutant allele demonstrated an increased efficiency of R193H mutant cTnI incorporation into the sarcomere over wild-type (WT) cTnI and a primary and unique evolution of a Ca^{2+} independent diastolic tone and acute cellular remodeling in the absence of changes in Ca^{2+} handling, a result not seen with other Ca^{2+} sensitizing molecules [22]. Given these results, RCM mutants may alter the predicted dosage of mutant gene product and may affect myocyte physiology differently under intact Ca^{2+} cycling conditions, particularly given the recent evidence that the interplay between Ca^{2+} handling and cardiomyopathy mutant sarcomeres is critical to the organ level outcome [23]. Thus, a key unanswered question is to determine the primary effects of RCM and HCM mutant cTnI alleles on intact cardiac myocyte physiology studied under physiologic Ca^{2+} handling conditions. Using acute genetic

engineering of in isolated adult rodent cardiac myocytes with intact SR function this comparative study was performed to elucidate the primary mechanisms of HCM and RCM mutant cTnI alleles. In addition, myocytes were isolated from a rabbit model in order to assess the interactions between mutant cTnI alleles and Ca^{2+} handling mechanisms that more closely resembles human myocyte physiology [24].

2. Methods

2.1 Generation of recombinant adenovirus

As previously described, WT and WT cTnI tagged with C-terminal flag epitope (DYKDDDDK, Sigma) was subcloned into a pGem3Z vector [25], which was then used to engineer five RCM-linked cTnI mutations, L145Q, R146W, A172T, K179E, and D191G, into the full-length rat cTnI cDNA using the Stratgene Quick Change site directed mutagenesis kit. The following oligonucleotide primers were used for mutagenesis (IDT; Coralville, IA): L145Q Sense 5'-GGCAAGTTTAAGCGGCCCACTCAGCGAAGAGTGAGAATCTc-3' Anti-sense 5'-GAGATTCTCAGTCTTCGCTGAGTGGGCCGCTTAAACTTGCC-3'; R146W Sense 5'-GCGGCCCACTCTCTGGAGAGTGAGAATCTCAGC-3' Anti-sense 5'-GCTGAGATTCTCACTCTCCAGAGAGTGGGCCGC-3'; A172T Sense 5'-CCTTGGACCTGAGGACCCACCTCAAGCA GG-3' Anti-sense 5'-CCTGCTTGAGGTGGGTCCT CAGGTCCAAGG-3'; K179E Sense 5'-CCTCAAGCAGGT GAAGGAGGAGGACATTGAGAAGG-3' Anti-sense 5'-CCTTCTCAATGTCCTCCTCCTTCACCTGCTTGAGG-3'; D191G Sense 5'-CCGGGAGGTGGGAGGCTGGCGCAAGAATATCG-3' Anti-sense 5'-CGATATTCTTGCGCCAGCCTCCCACCTCCCGG-3'. All cTnI mutants were confirmed by sequencing using the following primer sets: T7, SP6 and 2 custom primers (upstream 5'-GCCGGCGCCTGCTCCTGT-3' and downstream 5'-CTTTCGGCCTTCCATTCCACTTAG -3'). To generate recombinant viral vectors, the mutant cTnIs were subcloned with and without C-terminal flag epitope into the pDC315 AdMax shuttle vector (Microbix Biosystems Inc.). Viral particle lysates were prepared for infection of a cell factory and plaque assays were used for determining the viral titer [22]

2.2 Adult cardiac myocyte isolation and primary culture

Rat hearts were excised for retrograde perfusion from heparinized (1500 U/kg) and anesthetized (Nembutal; 150 U/kg) adult female Sprague Dawley rats (200g, Harlan, Indianapolis, IN). The care and use of the laboratory animals for this study were in agreement with the guidelines set forth by the University of Michigan Committee on the Use and Care of Animals. Veterinary care was provided by the University of Michigan Unit for Laboratory Animal Medicine. Ventricular cardiac myocytes were isolated via collagenase-hyaluronidase digestion as previously described [26]. The average yield from rat myocyte isolations was 1.8×10^6 cells with 77% viability.

In companion studies, rabbit hearts were excised from heparinized (400 U/kg) and anesthetized (Nembutal; 65mg/kg) adult male New Zealand White rabbits (2.2–2.6kg, Harlan, Indianapolis, IN). Ventricular cardiac myocytes were isolated via collagenase-hyaluronidase, protease digestion as previously described [27]. Rabbit preparations resulted in an average yield of 5.9×10^6 cells with 50% viability.

Isolated myocytes were placed in serum-free DMEM and subsequently transduced with adenovirus containing recombinant cTnIs [26]. Adenoviral gene transfer to isolated myocytes was performed at an experimentally predetermined optimal multiplicity of infection (multiplicities of infection, MOI, 20) based on the stoichiometric cTnI replacement for each vector and level of efficiency.

2.3 Protein expression and Western blot analysis

To assess the mutant cTnIs expression and incorporation into the sarcomere, cultured ventricular myocytes samples were prepared for gel electrophoresis and Western blot analysis as previously described [25;28]. A flag epitope monoclonal antibody (MAB) (M2, 1:1000, Sigma) and a cTnI specific polyclonal antibody (AB1627, 1:1000, Chemicon) were used for immunodetection, and horseradish peroxidase-conjugated goat anti-mouse or goat anti-rabbit secondary antibodies were used for chemiluminescence detection (1:2000, Amersham).

2.4 Localization and incorporation of mutant cTnI by immuno-fluorescence and confocal microscopy

Immunofluorescence techniques were performed as previously described [25;28]. Dual labeling of myocytes used a primary monoclonal antibody directed against the flag epitope (M2, 1:500, Sigma) detected by a Texas Red-conjugated mouse IgG secondary antibody (1:100, Molecular Probes) in addition to a second primary antibody directed against α-actinin (EA53, 1:500, Sigma) and detected by Alexa 488-conjugated mouse IgG secondary antibody. The MIAC Olympus FV500 confocal microscope (University of Michigan Diabetes Core) provided high resolution visualization of myocyte immunofluorescence.

2.5 Steady-state calcium activated isometric force measurements

Ca^{2+} activated isometric force measurements were performs on single, rod-shaped, permeabilized cardiac myocytes as previously described [29]. Solution pH was adjusted to 7.00 (or 6.20 for acidic pH experiments) with KOH/HCl. Relaxing solution (RS) pCa (−log [Ca^{2+}]) was 9.0 and maximal activating solution (AS) pCa was 4.0. Initial sarcomere length was set at 2.1 μm and the isometric tension-pCa relationship was determined by measuring isometric tension generation in response to various levels of Ca^{2+} activation ranging from nominal Ca^{2+} (pCa=9.0) to maximal (pCa=4.0) Ca^{2+} concentrations [29]. The Hill coefficient (n) and pCa_{50} were determined with a nonlinear least squares fitting algorithm. The catalytic subunit of PKA was used for phosphorylation studies as previously described [30].

2.6 Intact cardiac myocyte contractility and calcium transients

Sarcomere length measurements and intracellular Ca^{2+} transients were measured simultaneously at 37°C using the Ionoptix system (Ionoptix Co., Milton, MA) as previously described [22;31]. Myocytes were electrically paced at 40 volts with a frequency of 0.2 Hz. Ca^{2+} transient measurements were accomplished using the Ca^{2+} indicator, Fura-2 AM (5 μM [Fura-2], Molecular Probes by Invitrogen). Some experiments utilized pairwise comparisons of myocytes ± 10μM Diltiazem (Sigma). For stimulation-frequency experiments, pacing frequency was varied from 0.2, 0.5, 1.0 to 2.0 Hz for rat and 0.5, 0.75, 1.0 to 2.0 Hz for rabbit myocytes. At each frequency a minimum of 12 contractions was used for the myocyte to achieve a steady state, and the average of 8 subsequent contractions was used for analysis [22;31].

2.7 Statistical Analysis

Data are reported as mean ± SEM and statistical analyses were performed using Prism4 (Graph Pad, San Diego, CA). ANOVA and Newman Keuls post hoc analysis was used for statistical comparisons for multiple experimental groups. T-test was used for pairwise analysis of diltiazem's effects on myocyte function.

3. Results

3.1 Targeted stoichiometric replacement and sarcomeric incorporation of RCM and HCM mutant cTnIs in adult cardiac myocytes

Virally transduced HEK (human embryonic kidney) 293 cells, which are devoid of endogenous cTnI, were collected for Western blot analysis and probed with a cTnI specific antibody ~48 hours post gene transfer. Transduction with identical viral concentrations resulted in equivalent protein expression of each mutant cTnI (Figure 1B) when normalized to silver stain as a loading control. Isolated adult rat cardiac myocytes, transduced with adenoviral vectors carrying mutant cTnI constructs, were examined for cTnI expression over time in culture from days two through four after gene transfer. All mutant and WT cTnI constructs were engineered with a C-terminal flag epitope tag in order to distinguish recombinant from native cTnI by molecular weight. In this and previous studies, the epitope tagged cTnI had no detected effects on myocyte structure and function [22;25;32], and there were no significant functional differences between flag and non-flag mutant cTnI (t-test, $P>0.05$). Western blot analysis with a cTnI specific antibody showed a time dependent increase in flag tagged mutant cTnIs and concomitant decrease in native cTnI expression in the absence of changes in other myofilament proteins (Figure 1B). This result was quantified by densitometry over multiple preparations (Figure 1C and D). The average percent replacement varied at each time point and between mutants where mutations in the helix 4 domain (H4, Figure 1A and C) had the highest level of replacement at each time point (Figure 1D). Myocyte function was primarily examined four days post gene transfer when the average replacement of mutant cTnIs in the H4 region was 67±6% and those in the inhibitory region (IR) was 33±2% (Figure 1A and D). The D191G mutant attained 45 ±5% replacement, which closely paralleled the temporal replacement of flag tagged WT cTnI (Figure 1D). This experiment demonstrated that cTnI stoichiometry is tightly maintained despite an overexpression of cTnI message. This provides further evidence that this gene transfer model is one of replacement as previously described [22;25;28]. To further support this result the relative replacement mutant cTnI was compared between intact (I) and membrane permeabilized (P) myocyte preparations (Figure 1E). Cardiac TnI content and the percent replacement of native cTnI between intact and permeabilized myocytes were not significantly different (Figure 1E) indicating that epitope tagged mutant cTnIs are stoichiometrically replacing the native cTnI and not accumulating in the cytosol.

The comparatively low level of stoichiometric replacement achieved with the IR mutant cTnIs (RCM L145Q, R146W, and HCM R146G) raised the possibility that IR domain mutant cTnIs are at a disadvantage when competing for sites on the myofilaments relative to WT cTnI. To test this hypothesis, thin filament competition assays were performed in cardiac myocytes to determine if adenoviral vector-mediated WT cTnI (non-flagged) would effectively out-compete the IR mutant cTnIs for sites on the sarcomere (Figure 1E). Adult rat cardiac myocytes were co-transduced with increasing titers of WT cTnI (0 – 500 MOI) and either epitope tagged RCM-linked L145Q or R146W cTnI held at a fixed titer (20 MOI) and collected for Western blot four days post gene transfer. At a titer of 50 MOI, WT cTnI had already limited the incorporation of L145Q and R146W into the sarcomere, and at 500 MOI of WT cTnI both L145Q and R146W had minimal replacement (Figure 1E) similar to previous reports from competition assays performed with the HCM linked mutant R146G [25]. These competition assays demonstrate that the IR mutant cTnIs are at a disadvantage relative to WT cTnI when incorporating into the sarcomere. This is in contrast to the recent report that RCM R193H cTnI significantly out-competed WT cTnI and preferentially incorporated into the intact sarcomere [22].

Incorporation and localization of the mutant cTnIs into the cardiac sarcomere was also assessed by immunohistochemistry and confocal imaging at four days post gene transfer. Scoring of rod-shaped myocytes positive for flag epitope labeling indicated that >95% of the myocytes

incorporated mutant cTnIs, underscoring the high efficiency of this approach. Dual labeling with monoclonal antibodies directed against α-actinin and the flag epitope tag established that mutant cTnIs, as represented here by A172T and D191G mutant myocytes, incorporated and localized appropriately into the sarcomere (Figure 1F). Single labeling with a polyclonal cTnI antibody showed a striated pattern similar to that obtained with flag epitope labeling, indirect evidence that the mutant cTnIs were localizing to the sarcomere and cTnI stoichiometry was maintained (*data not shown*).

3.2 RCM linked C-terminus mutant cTnIs further sensitize the myofilaments to Ca^{2+} relative to other mutants

Four days post gene transfer steady-state Ca^{2+} activated isometric tension was measured in single membrane permeabilized rodent myocytes. Representative isometric tension curves from WT and RCM mutant A172T myocytes (Figure 2A) illustrate the developed tension in response to low and maximal activating [Ca^{2+}] conditions. Under basal conditions, maximal tension generation was not different between groups (*data not shown*). The C-terminal RCM mutant cTnIs, A172T, K179E, and D191G, had higher pCa_{50} values (Figure 2B), indicating these mutants cause a significant increase in myofilament Ca^{2+} sensitivity of tension. HCM and RCM mutations in cTnI's IR domain had little effect on myofilament Ca^{2+} sensitivity of tension with 35% replacement (Figure 2B). Ca^{2+} activated tension generation was also measured under acidic conditions (Figure 2C, pH 6.2). Only the RCM A172T mutant myocytes retained an increased Ca^{2+} sensitivity of tension relative to WT with a drop in pH (Figure 2C, pH 6.2). The PKA catalytic subunit caused a similar rightward shift in the tension-pCa relationship in both WT (Figure 2D) and RCM mutants as represented by K179E mutant myocytes (Figure 2E). A small survey of WT and several RCM mutant myofilaments demonstrated that the magnitude of PKA-mediated desensitization was similar among all groups (Figure 2F). These data show that RCM mutant cTnI retain the ability to be desensitized by PKA mediated serine phosphorylation in order to facilitate faster relaxation.

3.3 RCM linked mutations in cTnI's Helix-4/C-terminal domain slow relaxation and Ca^{2+} transient decay rate

For all unloaded functional assays, non-transduced myocytes and myocytes adenovirally transduced with WT cTnI and flag epitope tagged cTnI were combined into one group (labeled control) because their functional outcomes for all mechanical measurements were not statistically different (ANOVA, $P>0.05$). Contractile function and Ca^{2+} transients were simultaneously measured in intact adult rat cardiac myocytes at physiologic temperature (37° C). A summary of contractility and Ca^{2+} transient parameters is presented in Table 1. Figure 3 shows representative sarcomere shortening (Figure 3A, left panel) and Ca^{2+} transients (Figure 3A, right panel) normalized to the peak shortening or Ca^{2+} amplitude. Figure 3A demonstrates the marked slowing of sarcomere length relaxation and Ca^{2+} transient decay in RCM linked helix-4/C-terminal domain mutant myocytes (represented by A172T) relative to myocytes with cTnI mutations in the IR domain (represented by R146G). IR domain mutant myocytes only displayed a slowing of relaxation/ fluorescence decay in the later phase of relaxation. Figure 3B summarizes the time from peak shortening/ fluorescence to 90% relaxation/decay for all of the cTnI mutations described. All of the helix-4/C-terminal domain RCM cTnI mutants caused a significant slowing at 50, 75, and 90% relaxation (Table 1). The RCM linked IR mutant myocytes were significantly slower to relax but not to the same extent as C-terminus mutants (Table 1). The HCM linked R146G mutant had a significant slowing of relaxation time relative to control only late in relaxation (Table 1, Figure 3B). To determine whether the variation between mutant relaxation times was due to different levels of replacement, the relationship between time to 90% relaxation and magnitude of cTnI replacement was measured in both A172T and R146G myocytes (Figure 3C). Even at lower levels of replacement similar to that in R146G myocytes, A172T mutant myocytes had slower relaxation times relative to

R146G mutant myocytes (Figure 3C,left panel, A172T, R^2=0.99, y=0.0015X+0.171, R146G, R^2=0.71, y=0.0014X+0.116). The cTnI flag myocytes had no change in relaxation time with increasing incorporation of cTnI flag (Figure 3C, left panel, R^2=0.12, y=5.0E−05X+0.128). Figure 3C (right panel) demonstrates that at similar or reduced levels of replacement A172T (10% replacement) significantly slows relaxation time relative to R146G (20% replacement) mutant myocytes. Together these data indicate that at similar low levels of replacement the helix-4/C-terminal RCM mutant, A172T, still has a greater effect to slow relaxation than IR domain mutants.

The magnitude of change in relaxation time varied within the RCM group as well as between RCM and HCM myocytes (Table 1, Figure 3B). Overall, the helix-4/C-terminal domain mutant cTnI myocytes were slower to relax than those containing IR domain mutant cTnIs independent of RCM/HCM linkage. This slowing of sarcomere relaxation is most likely due to the significant increase in myofilament Ca^{2+} sensitivity caused by helix-4/C-terminal domain mutant cTnIs. Post hoc analysis between IR mutants, with similar levels of replacement, showed that the RCM mutant myocytes are significantly slower to relax compared to HCM R146G mutant myocytes at 50 and 75% relaxation time but not at 90% (Table 1) where they were all equally slow. Previous studies demonstrated the restitution of Ca^{2+} handling protein expression, hemodynamic function, and abrogation of the hypertrophic response in a mouse model of HCM after chronic administration of the Ca^{2+} channel blocker, diltiazem [23;33]. We therefore tested the hypothesis that diltiazem would correct slowed relaxation kinetics evident in HCM and RCM myocytes. Diltiazem significantly blunted sarcomere shortening and Ca^{2+} transient amplitudes in all groups (Supplement Figure 1) and slowed relaxation in control and HCM myocytes but not in the already slow A172T myocytes (Supplement Figure 1). These data suggest that, unlike control and HCM R146G myocytes, RCM A172T cTnI increases the myofilament's Ca^{2+} sensitivity to such a high level that diltiazem does not elicit an additive response.

Overall, HCM and RCM mutant myocytes did not significantly affect sarcomere shortening or peak systolic Ca^{2+} amplitudes with the exception of RCM K179E myocytes that had larger shortening amplitudes (Figure 3C). Unique to the RCM K179E was a significantly blunted Ca^{2+} transient amplitude (Figure 3D), suggesting that this mutation causes a gain in contractility not seen in any of the other tested mutants. Resting sarcomere length in all of the experimental groups was significantly shorter than control myocytes (Figure 3D, left panel) in the absence of changes in diastolic Ca^{2+} (Figure 3D, right panel), suggesting a relative heightened level of basal actin-myosin interaction under resting/diastolic conditions.

3.4 Pacing causes an uncoupling between mechanics and Ca^{2+} handling in RCM but not HCM myocytes

Based on baseline mechanical measurements (Table 1 and Figure 3B), A172T and R146G mutant myocytes were selected as representative of RCM and HCM respectively for frequency-response experiments. Pacing frequency was gradually increased every 15 contractions over the following frequencies: 0.2 (basal), 0.5, 1.0, and 2.0 Hz as shown in the representative normalized raw sarcomere length traces in Figure 4A. Frequency-response experiments highlighted a significant frequency-dependent diastolic dysfunction in A172T mutant myocytes, which is illustrated in the representative mechanical transients shown as a function of frequency in Figure 4A (right panel). The dashed red lines in Figure 4A (right panel) represent the average diastolic sarcomere length at each frequency once steady state is achieved. The corresponding diastolic Ca^{2+} transients were also measured. A172T mutant sarcomeres were significantly shorter during relaxation throughout a train of pulses relative to controls. This effect became more pronounced as the frequency was increased, suggesting that these mutant myofilaments only partially relax as pacing escalates. To quantify this effect, the

average diastolic sarcomere lengths and fluorescence ratios were measured at each frequency >0.2 Hz. These values were subtracted from the diastolic sarcomere length/fluorescence ratio measured at 0.2 (Figure 4B). Unlike the A172T mutants, control and R146G mechanical transients remained tightly coupled to the Ca^{2+} transient. Control myocytes were able to fully relax and cycle Ca^{2+} despite increasing frequency (Figure 4A and B), but R146G myocytes yielded a frequency-dependent increase in diastolic Ca^{2+} (Figure 4B, right panel) and corresponding shortening of diastolic sarcomere length (Figure 4B, left panel). Ca^{2+} cycling occurs normally in the hyper Ca^{2+} sensitized A172T myocyte (Figure 4B), but with escalations in pacing frequency the A172T mutant myocytes developed a mechanical tone that was independent of [Ca^{2+}] during diastole (Figure 4B), a result similar to that reported in RCM R193H myocytes [22].

Additionally, frequency-response experiments demonstrated that both A172T and R146G myocytes (Figure 4C,D) behaved similarly and showed a typical negative staircase effect [34] as found for WT myocytes (Control, Figure 4C,D). Escalations in pacing frequency also accelerated sarcomere length relaxation and Ca^{2+} transient decay time (*data not shown*) in both A172T and R146G myocytes similar to controls.

3.6 RCM and HCM mutant cTnIs slow relaxation and Ca^{2+} decay to similar magnitudes in rabbit cardiac myocytes

In order to elucidate the physiologic effects of RCM and HCM mutant cTnI on myocyte function in a cellular system with Ca^{2+} handling properties resembling that of human adult cardiac myocytes [24], adult rabbit cardiac myocytes were acutely isolated for primary culture and adenovirally transduced with a subset of cTnI mutations including A172T (RCM archetype based on rodent measurements), R146G (HCM archetype), or flag tagged WT cTnI. To compliment our previously published work on adult rat cardiac myocytes acutely engineered with RCM mutant R193H cTnI [22], adult rabbit myocytes transduced with R193H cTnI are also included in this comparative analysis. Similar to rat, targeted stoichiometric replacement of the native cTnI for recombinant mutant cTnI in rabbit cardiac myocytes was measured by Western blot (Figure 6A) in which a time dependent increase in endogenous cTnI replacement was observed (Figure 6A). In the rabbit system, the IR mutant R146G replacement was 67% by day four in culture (Figure 6A, right panel), which is elevated relative to the replacement of this mutant obtained in the rat (Figure 1B). In comparison, A172T and R193H cTnI replacement approached 80% at the same time point (Figure 6A, right panel), a replacement similar to that obtained in rat myocytes (Figure 1B). Functional testing on isolated rabbit myocytes was performed on day four in culture when the levels of replacement were not statistically different between experimental groups ($P=0.092$, *ANOVA*).

Contractile function and Ca^{2+} transients were simultaneously measured in unloaded intact adult rabbit cardiac myocytes at physiologic temperatures (37°C). Resting sarcomere length was significantly shorter in the absence of elevated diastolic Ca^{2+} in R193H and A172T myocytes relative to control and R146G (Figure 6B). Similar to previously published data in the rat [22], the R193H had a greater effect to shorten resting sarcomere length when compared to other mutant cTnI alleles in the rabbit. All of the mutant cTnI myocytes had a significant decrease in Ca^{2+} transient amplitude (Figure 6C, right panel) in the absence of significant changes in shortening amplitude relative to control rabbit myocytes (Figure 6C, left panel). These data suggest that HCM and RCM mutant cTnI alleles have distinct effects on contractility in rabbit versus rat cardiac myocytes. In rat myocytes neither mutation affected shortening or Ca^{2+} transient amplitude (Figure 3C, [22]). Both A172T and R146G slowed rabbit myocyte relaxation to the same extent when compared to control myocytes (Figure 6D, left panel). The R193H mutant allele, however, significantly slowed rabbit myocyte relaxation beyond that of A172T and R146G (Figure 6D, left panel). In rabbit myocytes, the R193H cTnI allele exerted

dominant effects on mechanical relaxation as previously described in rat myocytes [22]. A172T and R146G mutants had a similar influence on rabbit myocyte relaxation which differs from the greater effect of A172T over R146G obtained in rat myocytes (Figure 3B). All three mutant cTnI alleles slowed the Ca^{2+} transient decay to a similar extent relative to control in rabbit cardiac myocytes (Figure 6D, right panel). This is in contrast to results obtained in the rat in which both R193H [22] and A172T (Figure 3B, right panel) have dominant effects to slow Ca^{2+} decay. These differences between mutant myocytes from rat versus rabbit could be due to the increased replacement of R146G obtained in rabbit myocytes or species related differences in Ca^{2+} handling.

4. Discussion

The identification of cTnI mutations causal for RCM or HCM immediately posed the problem of delineating whether primary structural and/or functional outcomes could generate the clinically distinct patient phenotypes associated with various forms of inherited cardiomyopathy [1;9]. This study reports the primary functional outcome of a gain in myofilament Ca^{2+} sensitivity and concomitant cellular diastolic dysfunction and Ca^{2+} transient remodeling due to the incorporation of inherited cardiomyopathy cTnI alleles in rodent and rabbit cardiac myocytes. Our main finding is that significant alterations in isolated myocyte function are (A) species-dependent and (B) allele-specific rather than segregating into distinguishing RCM versus HCM cellular phenotypes (Table 2). In rodent myocytes, RCM helix-4 mutant cTnI alleles had dominant effects when compared to HCM and RCM alleles in the IR domain of cTnI (Table 2). The modest effects on myofilament Ca^{2+} sensitivity and mechanical function of both RCM and HCM linked mutations in cTnI's IR domain is partially attributed to the finding that RCM mutations in the IR domain are disadvantaged when competing against WT cTnI for positions within the rodent cardiac sarcomere (Figure 1F). The mechanism by which IR mutant cTnI incorporation is hindered in the rodent myocyte is currently unresolved. Despite their poor incorporation, the IR cTnI mutants (R146W and L145Q cTnI) are acting as dominant-negatives as a relatively small percent replacement of the native cTnI for IR mutant cTnI caused a significant slowing of sarcomere relaxation both in the rat and rabbit acute gene transfer model (Table 1 and 2). HEK studies (Figure 1B) indicate that the mutant protein is translated and stable similar to control cTnI, and therefore poor incorporation of the L145Q and R146W mutants appears more related to structural alterations in the IR domain. These results suggest, in contrast to the ~50:50 ratio of WT to diseased protein content reported in hearts for other inherited cardiomyopathy alleles [35;36], individuals with one R146W or L145Q allele may be predicted to have relatively small amounts of mutant cTnI protein content in the sarcomere. By contrast, transduced rabbit myocytes, a model system in which IR and C-terminal domain mutants have equal capacity for replacement, demonstrated that both RCM linked A172T and HCM linked R146G myocytes slow relaxation to similar extents (Table 2). The RCM linked R193H cTnI allele [22], however, still exerted a dominant effect relative to other cardiomyopathy mutants to slow relaxation and elevate diastolic tone independent of species (Table 2). Collectively, these findings support a model where phenotypic outcome is both allele-specific and species-dependent indicating that the primary effects of cardiomyopathy linked cTnI alleles in our model system are not readily segregated into distinct inherited cardiomyopathy subtypes as suggested by the newly broadened contemporary definition of inherited cardiomyopathies [1].

The acute genetic engineering models used here enabled direct comparisons between cTnI mutant alleles at the intact myocyte level. The RCM linked R193H allele caused significant slowing of mechanical relaxation and elevated diastolic tone in rabbit myocytes (Figure 6) relative to A172T (RCM) and R146G (HCM) similar to the previous reports of rat cardiac myocytes acutely engineered with this mutation [22]. These results suggest that the R193H mutation stands apart as having its own distinguishing mechanical phenotype in both species.

With that exception, the rabbit model also highlighted the new finding that, unlike in rat myocytes, HCM and RCM cTnI mutants, directly slowed relaxation and Ca^{2+} transient decay time to the same extent when incorporated at similar high levels of replacement (Table 2). R146G served as the archetype for HCM in this study as it has the greatest functional deficits relative to other HCM mutations when R146G replacement is relatively high [16;20;21;25]. Previous reports from R146G transgenic mouse and rabbit models show that low levels of R146G replacement produce a mild phenotype and have a small effect on myofilament Ca^{2+} sensitivity of tension similar to reports here in rodent myocytes [18;37]. In both R146G transgenic mouse and rabbit models high levels of replacement are lethal suggesting a low tolerance for this mutant cTnI allele at the organismal level [18;37]. Interestingly, myocytes isolated from the R146G transgenic rabbit had normal relaxation with faster Ca^{2+} transient decay [37], opposite the results reported here for acutely engineered R146G rabbit myocytes. The differences between models are likely due to adaptive changes in NCX function that compensate for the altered myofilament Ca^{2+} sensitivity in the R146G transgenic rabbit [37]. Furthermore, while heightened R146G replacement could account for the effects on relaxation in intact rabbit but not rat myocytes measured here, studies in rat myocytes indicated, that even at similar replacement, A172T still had a greater effect on myocyte relaxation (Figure 3C). Previous experiments utilizing permeabilized reconstitution preparations found that RCM mutants in general had a greater effect to increase myofilament Ca^{2+} sensitivity relative to HCM mutants including R146G corroborating the dominant effect of A172T over R146G, [20;21]. Taken together these results suggest that species differences rather than gene dosage alone are directly influencing the primary functional outcome in intact cardiac myocytes.

A fundamental difference between rodent and rabbit myocytes is the inherent Ca^{2+} removal mechanism. In rodent cardiac myocytes, Ca^{2+} removal from the cytosol is almost exclusively driven by the SR's Ca^{2+} ATPase pump (SERCA, 92%); whereas, in rabbit and other larger mammals including humans, the Na^{+}-Ca^{2+} exchanger (NCX) has a greater contribution to Ca^{2+} extrusion from the cytosol (NCX, ~30%; SERCA, ~70%) [24]. Notably, the magnitude of delay in Ca^{2+} decay time was the same for all of the mutant myocytes such that R193H = A172T = R146G > WT (Figure 6D, right panel) despite the dominant effect of the R193H cTnI allele to slow rabbit myocyte relaxation beyond that of the mechanically slow A172T and R146G myocytes. This is in contrast to the rat in which the hierarchy of slowing both mechanical relaxation and Ca^{2+} decay time was as follows: R193H > A172T > R146G = WT (Table 1, [22]). Thus, we postulate that the enhanced contribution to cytosolic Ca^{2+} removal by NCX in rabbit myocytes [24] may be enough to equalize the effects of R193H, A172T, and HCM R146G myofilaments on Ca^{2+} handling (Figure 6D) but also critically influences the primary cellular phenotype. Recent evidence from a HCM transgenic mouse model [23] supports this hypothesis as altered Ca^{2+} handling played a role in cardiomyopathy disease pathogenesis. Additionally, myosin heavy chain (MHC) isoform could be contributing to the species-dependent functional outcomes as rat is αMHC dominant (fast motor) while rabbit is βMHC (slow motor) dominant [38;39]. The βMHC backbone of the rabbit myocytes slows cross-bridge cycling independent of Ca^{2+} [27], which may interact with the mutant cTnI alleles to further slow relaxation. The rabbit model in the present study further underscores the importance of understanding the primary effects of cardiomyopathy mutant alleles in larger mammals with Ca^{2+} handling mechanisms and myosin isoform profile that is comparable to humans.

Additionally, both acutely engineered HCM and RCM mutant rat (figure 3B) and rabbit (figure 5D) myocytes had significantly slowed Ca^{2+} transient decay time in addition to the direct effect of these alleles to slow myocyte relaxation. This altered Ca^{2+} transient decay could be directly related to the increased myofilament Ca^{2+} sensitivity of HCM and RCM mutant sarcomeres (figure 2). By directly increasing myofilament Ca^{2+} sensitivity with the acute expression of mutant cTnI alleles, we speculate that the myofilament's cytosolic Ca^{2+} buffering capacity, in

turn, is increased causing cytosolic Ca^{2+} removal to slow, similar to reports from HCM mutant cardiac troponin T alleles [40]. Heightened myofilament Ca^{2+} buffering could have severe down-stream consequences by augmenting Ca^{2+} cycling and becoming a potential substrate for arrhythmias [40], all of which have been associated with HCM in human patients [4;23].

This study demonstrates both in the rodent and more so in the rabbit isolated myocyte model that the primary effects of mutant cTnI alleles on cardiac myocyte physiology do not readily segregate into distinct phenotypes of HCM or RCM, but instead are allele and species specific. Overall, the differential cellular effects of cardiomyopathy-linked cTnI mutations are confounded by several variables at the cellular-level alone that include sarcomeric replacement, location of the mutation within cTnI's secondary structure, and species dependent differences in Ca^{2+} handling mechanisms. Inherited HCM and RCM are also both progressive diseases, so at the organismal-level, human disease phenotypes are further influenced by complex compensatory adaptations, environmental factors, and genetic modifiers [41;42]. A recent study of over a thousand patients from 16 families diagnosed with HCM found ~1.5% of these individuals had mutations in *TNNI3* or *MYH7* and functionally presented with restrictive cardiomyopathy underscoring the role of secondary factors in determining clinical outcomes [43]. Furthermore, within a cardiomyopathy classification like RCM there is a range of disease severity [9], which adds to the difficulty of clinically stratifying patients and further complicates understanding the pathogenesis from the cellular manifestations of a diseased allele to the clinical presentation. The evidence of phenotypic variability within kindreds and among patients with the same genotype [9;43;44], in addition to patients presenting with mixed RCM/HCM phenotypes [9] further support the notion that readily distinguishing between HCM and RCM is challenging and that RCM may fall under the broad clinical spectrum of HCM [1;43]. Together the data presented here show the inability to draw distinct physiologic lines between RCM and HCM cTnI alleles at the cell/molecular level. These complexities arise from species-dependent, genetic, and environmental interactions with specific cTnI alleles at the myocyte-level, and at the organ-level they likely combine to underlie the clinical manifestations of inherited cardiomyopathy reported in humans.

Supplementary Material

Refer to Web version on PubMed Central for supplementary material.

Acknowledgments

We thank Dr. Margaret Westfall, Dr. Sharlene Day, Dr. Todd Herron and Nathan Palpant for their helpful discussions, as well as Dustin Robinson for his expertise in culturing rabbit cardiac myocytes.

Sources of funding

This work was supported by the NIH and American Heart Association's Greater Midwest Predoctoral Fellowship.

Reference List

1. Maron BJ, Towbin JA, Thiene G, Antzelevitch C, Corrado D, Arnett D, Moss AJ, Seidman CE, Young JB. Contemporary definitions and classification of the cardiomyopathies: an American Heart Association Scientific Statement from the Council on Clinical Cardiology, Heart Failure and Transplantation Committee; Quality of Care and Outcomes Research and Functional Genomics and Translational Biology Interdisciplinary Working Groups; and Council on Epidemiology and Prevention. Circulation 2006;113:1807–1816. [PubMed: 16567565]
2. WHO. Report of the 1995 World Health Organization/International Society and Federation of Cardiology Task Force on the Definition and Classification of Cardiomyopathies. Circulation 1996;93:841–842. [PubMed: 8598070]

3. Braunwald E, Seidman CE, Sigwart U. Contemporary evaluation and management of hypertrophic cardiomyopathy. Circulation 2002;106:1312–1316. [PubMed: 12221045]
4. Maron BJ, Shirani J, Poliac LC, Mathenge R, Roberts WC, Mueller FO. Sudden death in young competitive athletes. Clinical, demographic, and pathological profiles. JAMA 1996;276:199–204. [PubMed: 8667563]
5. Fatkin D, Graham RM. Molecular mechanisms of inherited cardiomyopathies. Physiol Rev 2002;82:945–980. [PubMed: 12270949]
6. Maron BJ, Gardin JM, Flack JM, Gidding SS, Kurosaki TT, Bild DE. Prevalence of hypertrophic cardiomyopathy in a general population of young adults. Echocardiographic analysis of 4111 subjects in the CARDIA Study. Coronary Artery Risk Development in (Young) Adults. Circulation 1995;92:785–789. [PubMed: 7641357]
7. Rivenes SM, Kearney DL, Smith EO, Towbin JA, Denfield SW. Sudden death and cardiovascular collapse in children with restrictive cardiomyopathy. Circulation 2000;102:876–882. [PubMed: 10952956]
8. Kushwaha SS, Fallon JT, Fuster V. Restrictive cardiomyopathy. N Engl J Med 1997;336:267–276. [PubMed: 8995091]
9. Mogensen J, Kubo T, Duque M, Uribe W, Shaw A, Murphy R, Gimeno JR, Elliott P, McKenna WJ. Idiopathic restrictive cardiomyopathy is part of the clinical expression of cardiac troponin I mutations. J Clin Invest 2003;111:209–216. [PubMed: 12531876]
10. Farah CS, Reinach FC. The troponin complex and regulation of muscle contraction. FASEB J 1995;9:755–767. [PubMed: 7601340]
11. Takeda S, Yamashita A, Maeda K, Maeda Y. Structure of the core domain of human cardiac troponin in the Ca(2+)-saturated form. Nature 2003;424:35–41. [PubMed: 12840750]
12. Metzger JM, Westfall MV. Covalent and noncovalent modification of thin filament action: the essential role of troponin in cardiac muscle regulation. Circ Res 2004;94:146–158. [PubMed: 14764650]
13. Li MX, Wang X, Sykes BD. Structural based insights into the role of troponin in cardiac muscle pathophysiology. J Muscle Res Cell Motil 2004;25:559–579. [PubMed: 15711886]
14. Murakami K, Yumoto F, Ohki SY, Yasunaga T, Tanokura M, Wakabayashi T. Structural basis for Ca2+-regulated muscle relaxation at interaction sites of troponin with actin and tropomyosin. J Mol Biol 2005;352:178–201. [PubMed: 16061251]
15. Pirani A, Vinogradova MV, Curmi PM, King WA, Fletterick RJ, Craig R, Tobacman LS, Xu C, Hatch V, Lehman W. An atomic model of the thin filament in the relaxed and Ca2+-activated states. J Mol Biol 2006;357:707–717. [PubMed: 16469331]
16. Gomes AV, Potter JD. Cellular and molecular aspects of familial hypertrophic cardiomyopathy caused by mutations in the cardiac troponin I gene. Mol Cell Biochem 2004;263:99–114. [PubMed: 15524171]
17. Gomes AV, Liang JS, Potter JD. Mutations in human cardiac Troponin I that are associated with restrictive cardiomyopathy affect basal ATPase activity and the calcium sensitivity of force development. Journal of Biological Chemistry 2005;280:30909–30915. [PubMed: 15961398]
18. James J, Zhang Y, Osinska H, Sanbe A, Klevitsky R, Hewett TE, Robbins J. Transgenic modeling of a cardiac troponin I mutation linked to familial hypertrophic cardiomyopathy. Circ Res 2000;87:805–811. [PubMed: 11055985]
19. Takahashi-Yanaga F, Morimoto S, Ohtsuki I. Effect of Arg145Gly mutation in human cardiac troponin I on the ATPase activity of cardiac myofibrils. J Biochem (Tokyo) 2000;127:355–357. [PubMed: 10731705]
20. Yumoto F, Lu QW, Morimoto S, Tanaka H, Kono N, Nagata K, Ojima T, Takahashi-Yanaga F, Miwa Y, Sasaguri T, Nishita K, Tanokura M, Ohtsuki I. Drastic Ca2+ sensitization of myofilament associated with a small structural change in troponin I in inherited restrictive cardiomyopathy. Biochem Biophys Res Commun 2005;338:1519–1526. [PubMed: 16288990]
21. Kobayashi T, Solaro RJ. Increased Ca2+ Affinity of Cardiac Thin Filaments Reconstituted with Cardiomyopathy-related Mutant Cardiac Troponin I. J Biol Chem 2006;281:13471–13477. [PubMed: 16531415]

22. Davis J, Wen H, Edwards T, Metzger JM. Thin filament disinhibition by restrictive cardiomyopathy mutant R193H troponin I induces Ca2+-independent mechanical tone and acute myocyte remodeling. Circ Res 2007;100:1494–1502. [PubMed: 17463320]
23. Semsarian C, Ahmad I, Giewat M, Georgakopoulos D, Schmitt JP, McConnell BK, Reiken S, Mende U, Marks AR, Kass DA, Seidman CE, Seidman JG. The L-type calcium channel inhibitor diltiazem prevents cardiomyopathy in a mouse model. J Clin Invest 2002;109:1013–1020. [PubMed: 11956238]
24. Bers DM. Cardiac excitation-contraction coupling. Nature 2002;415:198–205. [PubMed: 11805843]
25. Westfall MV, Borton AR, Albayya FP, Metzger JM. Myofilament calcium sensitivity and cardiac disease: insights from troponin I isoforms and mutants. Circ Res 2002;91:525–531. [PubMed: 12242271]
26. Westfall MV, Rust EM, Albayya F, Metzger JM. Adenovirus-mediated myofilament gene transfer into adult cardiac myocytes. Methods Cell Biol 1997;52:307–322. [PubMed: 9379958]
27. Herron TJ, Vandenboom R, Fomicheva E, Mundada L, Edwards T, Metzger JM. Calcium-independent negative inotropy by beta-myosin heavy chain gene transfer in cardiac myocytes. Circ Res 2007;100:1182–1190. [PubMed: 17363698]
28. Michele DE, Albayya FP, Metzger JM. Thin filament protein dynamics in fully differentiated adult cardiac myocytes: toward a model of sarcomere maintenance. J Cell Biol 1999;145:1483–1495. [PubMed: 10385527]
29. Metzger JM. Myosin binding-induced cooperative activation of the thin filament in cardiac myocytes and skeletal muscle fibers. Biophys J 1995;68:1430–1442. [PubMed: 7787029]
30. Westfall MV, Turner I, Albayya FP, Metzger JM. Troponin I chimera analysis of the cardiac myofilament tension response to protein kinase A. Am J Physiol Cell Physiol 2001;280:C324–C332. [PubMed: 11208528]
31. Coutu P, Metzger JM. Genetic manipulation of calcium-handling proteins in cardiac myocytes. I. Experimental studies. Am J Physiol Heart Circ Physiol 2005;288:H601–H612. [PubMed: 15331372]
32. Day S, Davis J, Westfall M, Metzger J. Genetic engineering and therapy for inherited and acquired cardiomyopathies. Ann N Y Acad Sci 2006;1080:437–450. [PubMed: 17132800]
33. Westermann D, Knollmann BC, Steendijk P, Rutschow S, Riad A, Pauschinger M, Potter JD, Schultheiss HP, Tschope C. Diltiazem treatment prevents diastolic heart failure in mice with familial hypertrophic cardiomyopathy. Eur J Heart Fail 2006;8:115–121. [PubMed: 16214409]
34. Bers, DM. Excitation-Contraction Coupling And Cardiac Contractile Force. Netherlands: Kluwer Academic Publishers; 2001.
35. Cuda G, Fananapazir L, Zhu WS, Sellers JR, Epstein ND. Skeletal muscle expression and abnormal function of beta-myosin in hypertrophic cardiomyopathy. J Clin Invest 1993;91:2861–2865. [PubMed: 8514894]
36. Kimura A, Harada H, Park JE, Nishi H, Satoh M, Takahashi M, Hiroi S, Sasaoka T, Ohbuchi N, Nakamura T, Koyanagi T, Hwang TH, Choo JA, Chung KS, Hasegawa A, Nagai R, Okazaki O, Nakamura H, Matsuzaki M, Sakamoto T, Toshima H, Koga Y, Imaizumi T, Sasazuki T. Mutations in the cardiac troponin I gene associated with hypertrophic cardiomyopathy. Nat Genet 1997;16:379–382. [PubMed: 9241277]
37. Sanbe A, James J, Tuzcu V, Nas S, Martin L, Gulick J, Osinska H, Sakthivel S, Klevitsky R, Ginsburg KS, Bers DM, Zinman B, Lakatta EG, Robbins J. Transgenic rabbit model for human troponin I-based hypertrophic cardiomyopathy. Circulation 2005;111:2330–2338. [PubMed: 15867176]
38. Litten RZ, Martin BJ, Buchthal RH, Nagai R, Low RB, Alpert NR. Heterogeneity of myosin isozyme content of rabbit heart. Circulation Research 1985;57:406–414. [PubMed: 3161658]
39. Miyata S, Minobe W, Bristow MR, Leinwand LA. Myosin Heavy Chain Isoform Expression in the Failing and Nonfailing Human Heart. Circulation Research 2000;86:386–390. [PubMed: 10700442]
40. Knollmann BC, Kirchhof P, Sirenko SG, Degen H, Greene AE, Schober T, Mackow JC, Fabritz L, Potter JD, Morad M. Familial hypertrophic cardiomyopathy-linked mutant troponin T causes stress-induced ventricular tachycardia and Ca2+-dependent action potential remodeling. Circ Res 2003;92:428–436. [PubMed: 12600890]
41. Marian AJ. Modifier genes for hypertrophic cardiomyopathy. Curr Opin Cardiol 2002;17:242–252. [PubMed: 12015473]

42. Semsarian C, Healey MJ, Fatkin D, Giewat M, Duffy C, Seidman CE, Seidman JG. A polymorphic modifier gene alters the hypertrophic response in a murine model of familial hypertrophic cardiomyopathy. J Mol Cell Cardiol 2001;33:2055–2060. [PubMed: 11708849]

43. Kubo T, Gimeno JR, Bahl A, Steffensen U, Steffensen M, Osman E, Thaman R, Mogensen J, Elliott PM, Doi Y, McKenna WJ. Prevalence, clinical significance, and genetic basis of hypertrophic cardiomyopathy with restrictive phenotype. J Am Coll Cardiol 2007;49:2419–2426. [PubMed: 17599605]

44. Mogensen J, Murphy RT, Kubo T, Bahl A, Moon JC, Klausen IC, Elliott PM, McKenna WJ. Frequency and clinical expression of cardiac troponin I mutations in 748 consecutive families with hypertrophic cardiomyopathy. J Am Coll Cardiol 2004;44:2315–2325. [PubMed: 15607392]

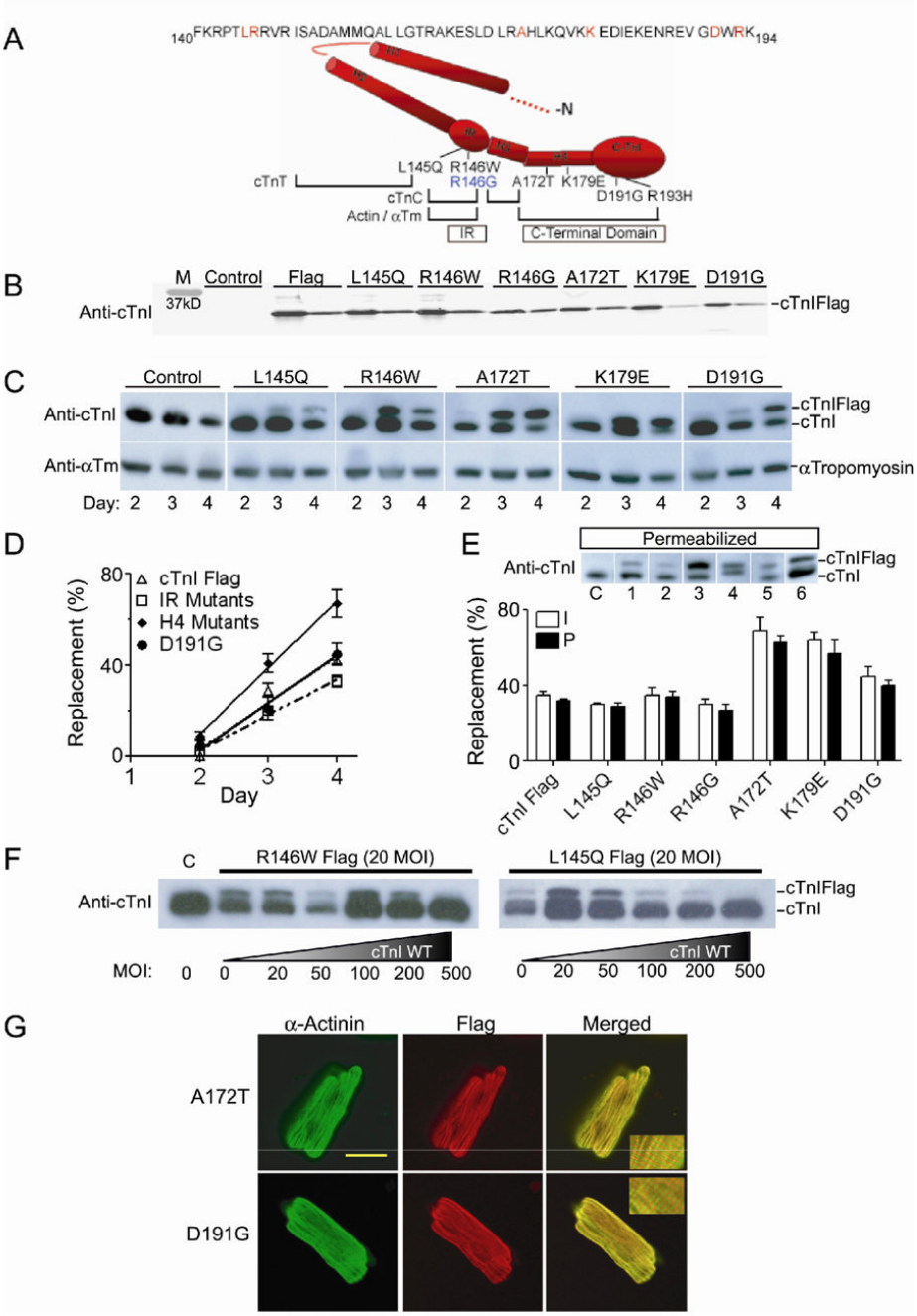

Figure 1. Targeted stoichiometric replacement and localization of mutant cTnIs in adult rat cardiac myocytes

(**A**) Schematic representation of cTnI's secondary structure and corresponding functional domains (H1, helix 1; H2, helix 2; IR, inhibitory region; H3, helix 3, H4, helix 4; and the C-terminal domain) and the corresponding amino acid sequence showing the location of RCM and HCM linked cTnI mutations. Beneath the structural schematic is an illustration of the regions of TnI that interact with other thin filament proteins critical to the regulation of cross-bridge cycling. (**B**) Representative Western blot showing the adenoviral mediated expression of mutant cTnIs and cTnI flag in HEK cells. Each group represents 2 lanes loaded with 5 and 1 μl of sample respectively and control represents non-transduced HEK cells. M = protein

standard marker (Biorad) (C) Representative Western blot showing the targeted stoichiometric replacement of native cTnI with epitope tagged mutant cTnI over 3 days starting at 2 days post gene transfer. Tropomyosin (αTm) was used as a loading control. There was no significant difference in myofilament stoichiometry across time as determined by cTnI/αTm ratios. (**D**) Summary of cTnI replacement with recombinant mutant cTnI as a function of time (IR mutants = the average replacement by L145Q, R146G, and R146W, open square; H4 mutants = the average replacement by A172T and K179E, closed diamond). (**E**) Summary of the average replacement attained for each individual mutant from membrane intact (I, white bar) and detergent permeabilized (P, black bar) at 4 days post gene transfer when functional measurements were made. Within a group there was no significant difference in percent replacement between intact and permeabilized myocytes, further evidence of mutant cTnI stoichiometric replacement (mean + SEM, t-test, n=5). The inset is a representative Western blot of membrane permeabilized control and mutant cTnI myocytes from 4 days post gene transfer. Lane C represents control myocytes and lanes 1–6 represent L145Q, R146W, A172T, K179E, D191G, and R146G mutants respectively. (**F**) Competition assay. Myocytes were co-transduced with flag epitope tagged L145Q or R146W (held at a constant titer, 20 MOI) and increasing viral titers of non-tagged WT cTnI (represented by the wedge, 0–500 MOI). WT cTnI out-competed the IR mutant cTnI for spots on the sarcomere around 100 MOI of WT cTnI. (**G**) Representative confocal projection images of isolated adult cardiac myocytes using dual labeling with anti-α-actinin antibody conjugated to Alexa 488 and anti-flag antibody conjugated to Texas Red. Images are shown for myocytes treated with adenovirus containing flag epitope tagged A172T and D191G mutant cTnI. The striated pattern labeling seen in the inset of merged image represents appropriate incorporation of the mutant cTnI. This striated labeling is representative of all the tested mutants. Bar = 20μm.

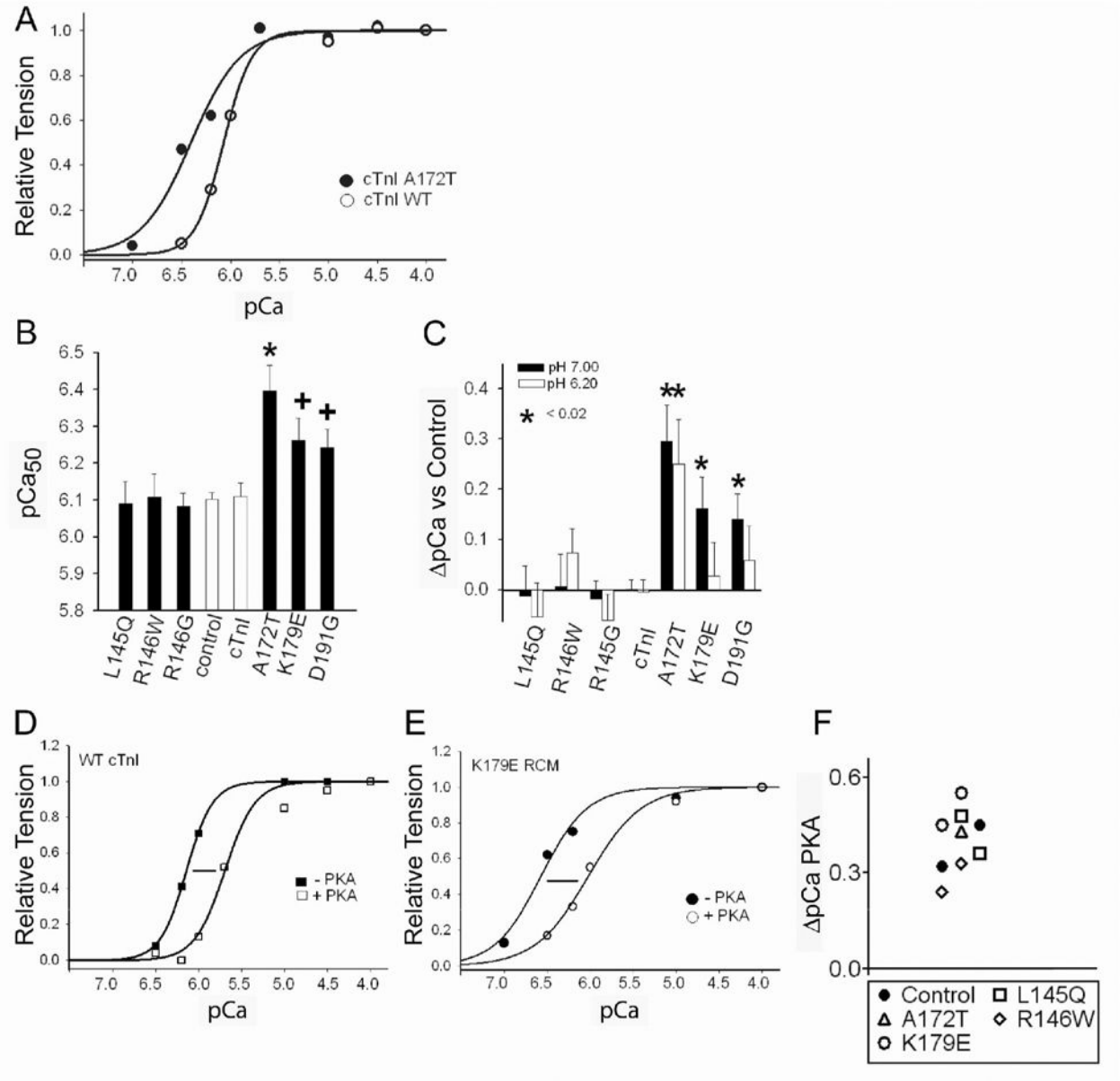

Figure 2. Ca^{2+} activated tension in single permeabilized RCM and HCM mutant cardiac myocytes

(**A**) Representative tension-pCa relationships for a wildtype (WT, open circle) and a RCM A172T (filled circle) myocyte. (**B**) Summary of myofilament Ca^{2+} sensitivity of tension generation (pCa_{50}) in adult WT, RCM, and HCM cardiac myocytes under basal conditions. Maximum tension generation (P_0, kN/m^2) was not significantly different between mutants (mean P_0 ± SEM, control 20.6±2.1, cTnI Flag 18.0±2.10, L145Q 25.0±3.7, R146W 21.5±4.8, R146G 14.9±1.5, A172T 20.6±2.6, K179E 17.6±2.2, D191G 17.0±1.7 kN/m^2). (**C**) Summary of the change in myofilament Ca^{2+} sensitivity of tension generation (pCa_{50}) relative to control at pH 7.0 and 6.2. cTnI represents WT cTnI treated myocytes. (**D**) Representative tension-pCa relationships for a WT myocyte under basal (−PKA, filled square) and PKA activating conditions (+PKA, open square). (**E**) Representative tension-pCa relationships for an RCM K1793 myocyte under basal (−PKA, filled circle) and PKA activating conditions (+PKA, open circle). Data represents mean + SEM, ANOVA and Newman Keuls post hoc analysis was used for statistical comparisons, * $P<0.001$ or * $P<0.05$ relative to control, n=7–8. (**F**) Summary of

the change in myofilament Ca^{2+} sensitivity of tension generation (pCa_{50}) between untreated and PKA stimulated conditions for mutant and control myocytes.

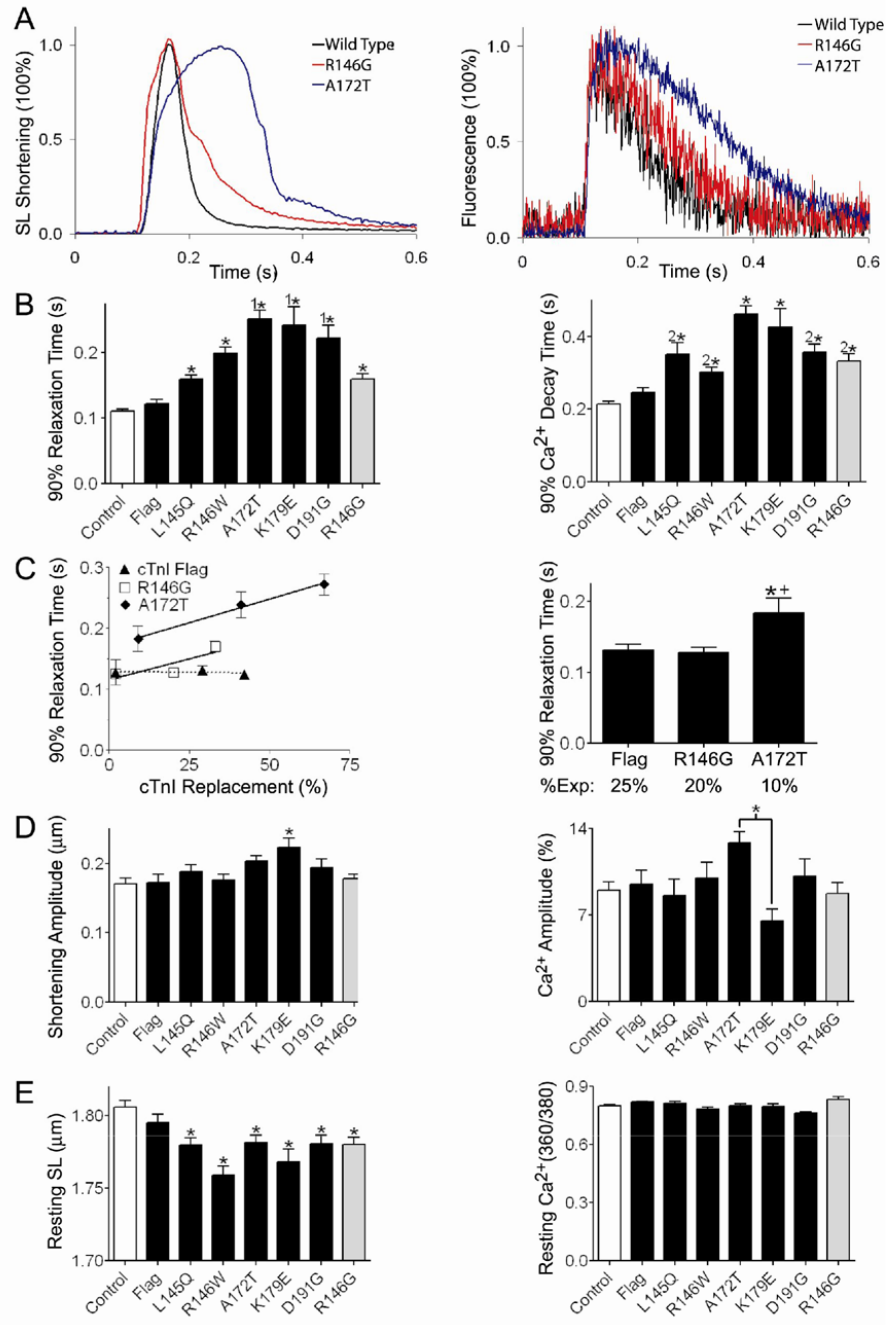

Figure 3. Intact single myocyte sarcomere length shortening and Ca^{2+} transients

(**A**) Representative raw sarcomere shortening (left panel) and the corresponding Ca^{2+} transients (right panel) from WT, R146G, and A172T transduced myocytes. Traces were normalized to peak shortening or the peak height of the Ca^{2+} transient to emphasize the mutant cTnI dependent slowing of relaxation and remodeling of the Ca^{2+} transient. (**B**) Summary of 90% sarcomere relaxation time (left panel) and the corresponding time to 90% Ca^{2+} transient decay (right panel). Relaxation and decay times were determined by calculating the difference from the time of peak shortening/fluorescence to 90% relaxation/decay. (C) Left panel: linear regression analysis of 90% relaxation time as a function of percent native cTnI replacement (A172T, R^2=0.99, y=0.0015X+0.171; R146G, R^2=0.71, y=0.0014X+0.116; cTnI flag,

R^2=0.12, y=5.0E-05X+0.128). Differing doses of cTnI replacement were obtained by studying myocytes a different time points. Right panel: a summary of 90% relaxation time for flag, R146G and A172T mutant myocytes at low levels of replacement (10–25%). At 10% replacement, A172T mutant myocytes are significantly slower to relax relative to R146G and flag myocytes. (**D**) Summary of sarcomere length shortening amplitude (left panel) and Ca^{2+} transient amplitude normalized to baseline fluorescence (right panel). (**E**) Summary of baseline sarcomere lengths (left panel) and resting Ca^{2+} for all of the experimental groups (right panel). All mechanical and Ca^{2+} transient values are expressed as mean + SEM, ANOVA and Newman Keuls post hoc analysis was used for statistical comparisons, * different from control and flag or between A172T and K179E as noted in (C) right panel, 1 different from all IR mutants, 2 different from A172T mutants, $P<0.05$, $n>35$.

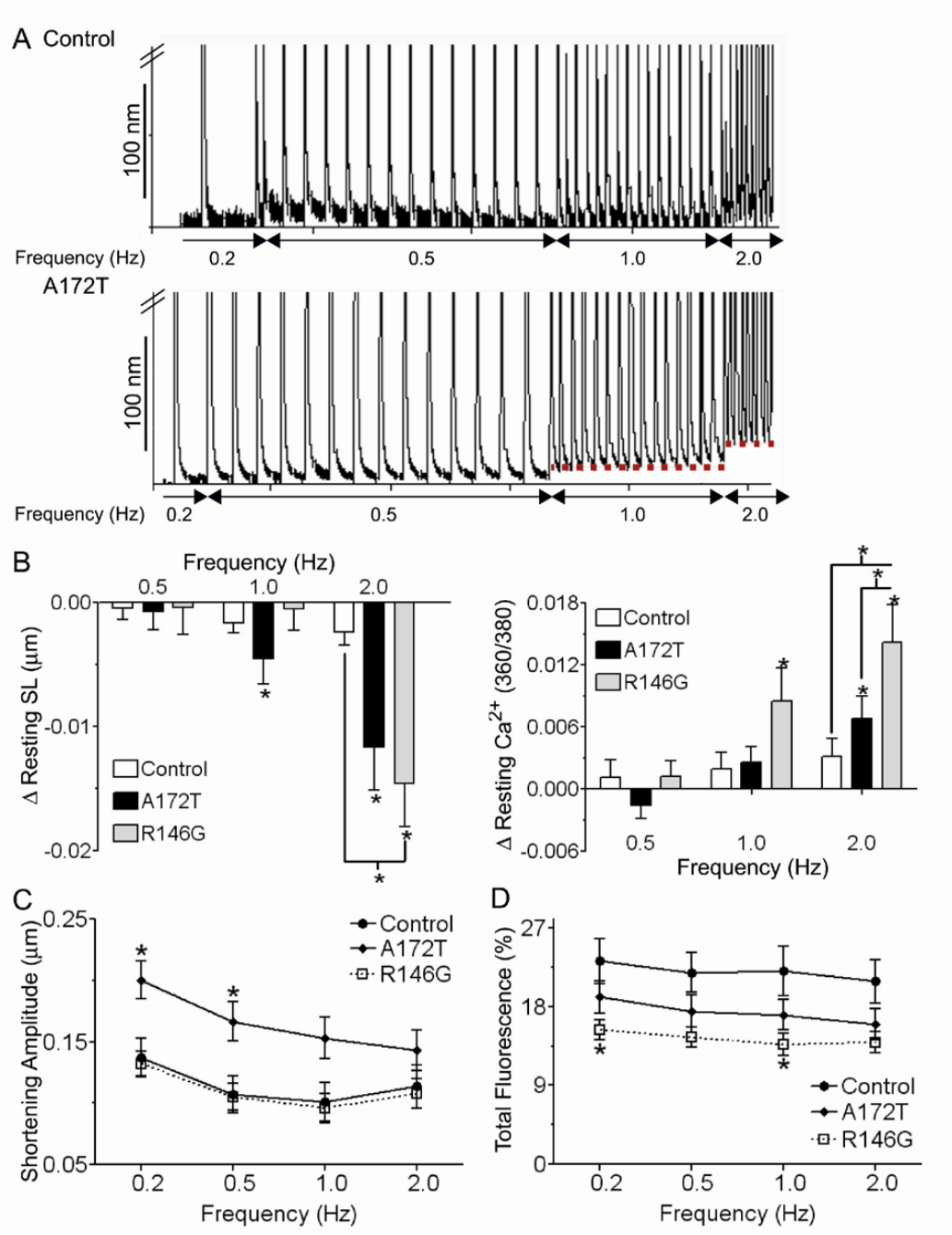

Figure 4. Frequency-dependent escalation in mechanical tone of A172T myocytes

(**A**) Representative stimulation-frequency traces of sarcomere shortening normalized to shortening amplitude measured at 0.2Hz for R193H mutant (left panel) and control (right panel) myocytes. Dashed red lines represent the change in diastolic sarcomere length delineated by frequency relative to prestimulation resting sarcomere lengths. (**B**) Summary of the average change in dynamic diastolic sarcomere length and the corresponding Ca^{2+} level at each frequency. Values (0.5–2.0 Hz) represent the change in sarcomere lengths from the dashed line to prestimulation resting sarcomere lengths at each frequency. (**C**) Summary of sarcomere shortening and (**D**) Ca^{2+} transient amplitude as a function of frequency. Values are expressed as mean + SEM, ANOVA per each frequency and Newman Keuls post hoc analysis was used

for statistical comparisons.* different from 0 (t-test), + different from control, # different from A172T (ANOVA per each frequency), $P<0.05$, n=25–30.

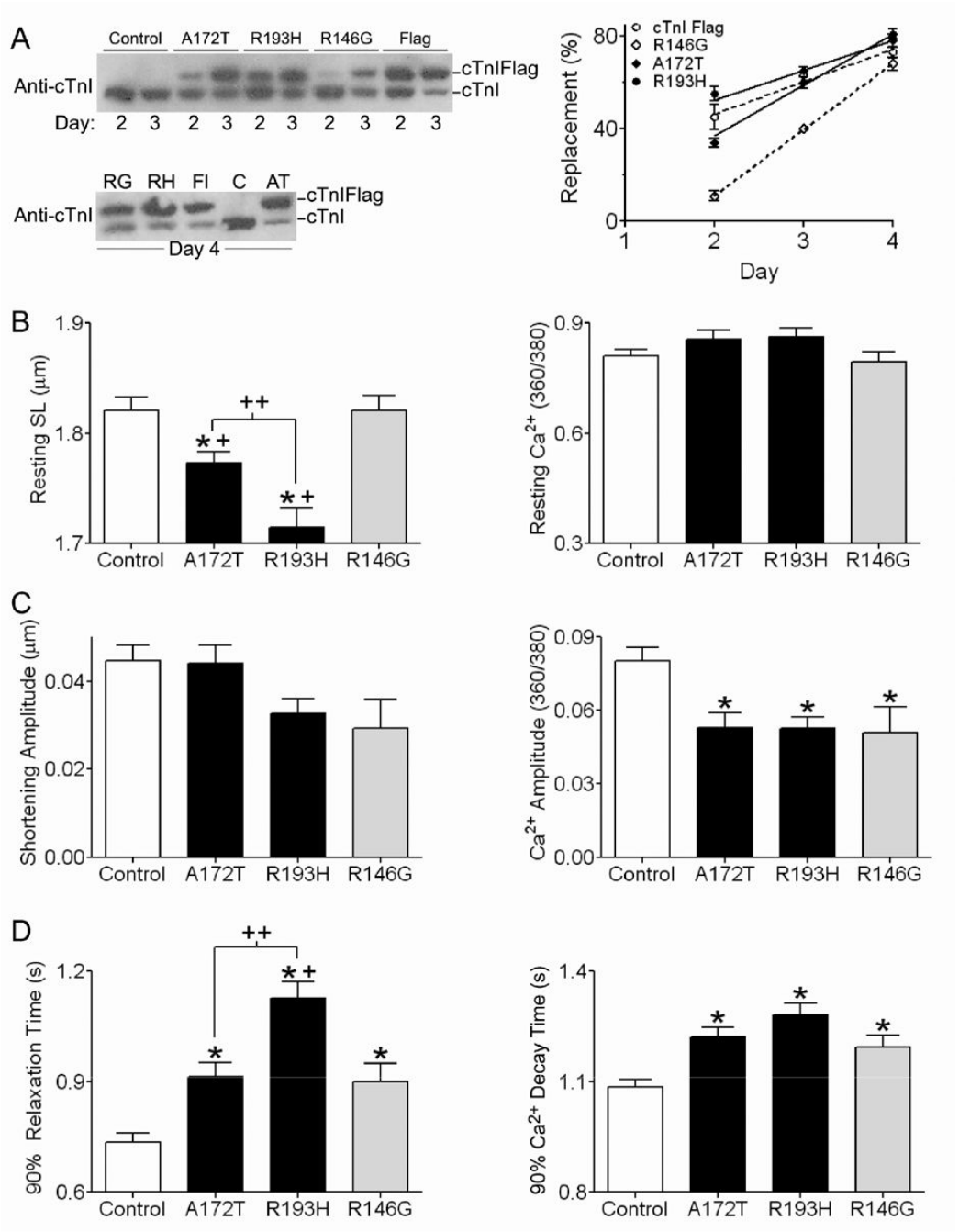

Figure 5. Targeted stoichiometric replacement of mutant cTnIs and functional outcome in adult rabbit cardiac myocytes

(**A**) Representative Western blots showing the targeted stoichiometric replacement of native cTnI with epitope tagged mutant A172T, R193H, R146G, and wild-type Flag cTnI at days two through three (top blot) and four days (bottom blot) post gene transfer as detected by a cardiac specific TnI antibody (left panel) and a summary of cTnI replacement with recombinant mutant cTnI as a function of time (right panel). Tropomyosin (αTm) was used as a loading control. There was no significant difference in myofilament stoichiometry across time as determined by cTnI/αTm ratios. (**B**) Summary of baseline sarcomere lengths (left panel) and resting Ca^{2+} for all of the experimental groups (right panel). (**C**) Summary of sarcomere length

shortening amplitude (left panel) and Ca^{2+} transient amplitude (right panel). (**D**) Summary of 90% sarcomere relaxation time (left panel) and the corresponding time to 90% Ca^{2+} transient decay (right panel). Relaxation and decay times were determined by calculating the difference from the time of peak shortening/fluorescence to 90% relaxation/decay. All mechanical and Ca^{2+} transient values are expressed as mean + SEM, ANOVA and Newman Keuls post hoc analysis was used for statistical comparisons, Post hoc tests: * different from control, + different from R146G, ++ different from A172T, $P<0.05$, $n>25$.

Table 1

Sarcomere length (SL) shortening measurements from single intact cardiac myocytes

WT is the control group consisting of combined data from non-transduced and AdcTnI wild-type myocytes. A t-test indicated WT and cTnI flag myocytes were not different across all parameters (P>0.1), thus the flag tag does not affect intact myocyte function. Shortening and relaxation velocity is normalized to the peak shortening amplitude. Relaxation time is calculated from peak shortening to 50, 75, or 90% of relaxation and ½ width is the time from 50% peak contraction to 50% relaxation. Values are represented as the mean + SEM, ANOVA and Newman Keuls post hoc analysis was used for statistical comparisons.

Myocyte mechanical measurements

	Baseline SL (μm)	**Amplitude (nm)**	***Dep vel* (%Amp)**	***Ret Vel* (%Amp)**	**50% RTP (ms)**	**75% RTP (ms)**	**90% RTP (ms)**	**½ Width (ms)**
WT	1.817 ± 0.005	172 ± 8.1	32.0 ± 1.1	18.5 ± 0.86	40 ± 2	70 ± 3	123 ± 5	73 ± 2
Flag	1.804 ± 0.006	192 ± 10.5	37.0 ± 1.8	20.8 ± 0.63	43 ± 2	72 ± 3	129 ± 5	79 ± 3
L145Q	1.776 ± 0.005*	188 ± 8.9	26.4 ± 1.3	17.2 ± 0.67	53 ± 2[2]	83 ± 4	159 ± 7*	107 ± 5*
R146W	1.759 ± 0.006*	177 ± 7.9	26.6 ± 1.1	13.1 ± 0.50*,#	65 ± 3*,#	112 ± 6*,#,3	200 ± 9*	110 ± 5*
A172T	1.781 ± 0.005*	204 ± 7.1	33.4 ± 1.7	13.0 ± 0.53*,#	73 ± 4*,#	130 ± 6*,#,3	252 ± 13*,1	118 ± 4*,#
K179E	1.768 ± 0.009*	223 ± 13.5*	27.4 ± 0.87	14.2 ± 0.93*,#	65 ± 7*,#	121 ± 1*,#,3	242 ± 29*,1	103 ± 6*
D191G	1.78 ± 0.005*	195 ± 11.6	29.5 ± 1.9	13.6 ± 0.85*,#	68 ± 6*,#	122 ± 1*,#,3	223 ± 15*,1	92 ± 5*
R146G	1.78 ± 0.005*	178 ± 7.2	27.1 ± 0.74	17.9 ± 0.50	46 ± 2	81 ± 4	160 ± 8*	92 ± 3*

Calcium transient measurements from single intact cardiac myocytes

	Baseline (360/380)	Amplitude (%BL)	*D vel* Ca^{2+} (% Amp)	*R Vel* Ca^{2+} (% Amp)	50% DTP (ms)	75% DTP (ms)	90% DTP (ms)	½ Width (ms)
WT	0.84 ± 0.007	12.6 ± 1.0	112 ± 6	14.0 ± 2.0	100 ± 5	166 ± 8	266 ± 14	132 ± 2
Flag	0.81 ± 0.010	13.1 ± 0.9	104 ± 7	16.2 ± 2.7	106 ± 5	170 ± 8	263 ± 13	129 ± 4
L145Q	0.81 ± 0.01	8.5 ± 1.3	110 ± 11	11.6 ± 3.2	128 ± 7[2]	229 ± 17*,#	350 ± 33*,2	124 ± 7
R146W	0.78 ± 0.009	10.0 ± 1.2	109 ± 11	11.4 ± 1.7	144 ± 6*,#	212 ± 8.4*,#	303 ± 12*,2	126 ± 9
A172T	0.80 ± 0.009	12.8 ± 0.9	109 ± 6	10.8 ± 0.9	169 ± 6*,#	257 ± 11*,#	461 ± 23*,#	184 ± 7*,#
K179E	0.79 ± 0.014	6.5 ± 0.9[2]	88 ± 7	10.1 ± 1.5	131 ± 9,[2]	222 ± 20*,#	427 ± 49*,#	141 ± 6
D191G	0.77 ± 0.008	10.2 ± 1.3	95 ± 7	8.0 ± 0.6	142 ± 6*,#,2	224 ± 11*,#	357 ± 23*,2	127 ± 4
R146G	0.82 ± 0.014	8.7 ± 0.9	111 ± 13	12.5 ± 1.9	107 ± 4	160 ± 7	333 ± 21*,2	140 ± 4

*Post Hoc effect relative to WT and flag

#P<0.05 Post Hoc effect relative to HCM R146G

1Post Hoc effect relative to all IR mutants

2Post Hoc effect relative to RCM A172T

3Post Hoc effect relative to RCM L145Q, ANOVA, P<0.05, n>35 myocytes.

Key: BL= baseline, Dep Vel = sarcomere length shortening velocity, Ret Vel = sarcomere length relaxation velocity, RTP = relaxation time from peak, D Vel Ca^{2+} = rate of rise of the Ca^{2+} transient, R Vel Ca^{2+} = Ca^{2+} transient decay rate, and DTP = Ca^{2+} transient decay time from peak.

Table 2

Comparison of the primary effects of RCM and HCM mutant cTnI alleles in rodent and rabbit cardiac myocytes

A summary of the primary effects of RCM and HCM mutant cTnI alleles on cardiac myocyte structure and function. The quantity of + signs represents the relative magnitude of change in function or replacement. A − sign represents no change relative to WT/control myocytes.

	Stoichiometric Replacement	Slow Relaxation	Diastolic Tone
Rodent			
HCM	+	+	+
RCM IR / Helix-4	+/+++	+/+++	+/++
Rabbit			
HCM	+++	+	−
RCM	+++	++	++
Rodent/Rabbit			
R193H*	+++	++++	++++

* indicates previously reported data from rat myocytes acutely engineered with RCM mutant R193H cTnI [22].